26th International Congress on Modelling and Simulation, Adelaide, SA, Australia, 30 Nov–4 Dec 2025
mssanz.org.au/modsim2025

Drift analysis of a SLAM-based handheld laser scanner in gully environments

E Rice [a] and R McCosker [a]

[a] *Department of the Environment, Tourism, Science and Innovation*
Email: edward.rice@detsi.qld.gov.au

Abstract: Drift in handheld laser scanners (HLS) has typically been assessed by comparison of the point cloud against a reference scan (e.g. from a terrestrial laser scanner) without consideration of how this drift changes as a function of time (scan duration). This study was carried out in a channel-like gully and measured drift in a SLAM-based HLS trajectory, rather than the point cloud, and aimed to determine the effect of scan duration and incorporating closed loops on drift severity in non-georeferenced scans. The study design included measuring drift at a mid-scan control point, which was revisited during scans. We hypothesise, this method inadvertently allowed the sensor's SLAM algorithm to correct for drift at the point we were attempting to measure it. As a result, we could not fully assess the aims of this study. Evaluating the effectiveness of mid-scan control points in reducing drift, compared to traditional closed loops, is worthwhile, as this may offer an alternative drift-reduction method in environments where closed loops are impractical, such as confined gullies with only a narrow walkable floor.

Keywords: *SLAM drift, handheld laser scanner, gully monitoring*

1. INTRODUCTION

Fine sediment from gullies adversely impacts the landscape and the health of receiving waterbodies, including water quality of the Great Barrier Reef (GBR) lagoon (Bartley et al. 2014, Koci et al. 2020, Lamane et al. 2025, Waterhouse et al. 2024). Detecting geomorphic change and measuring erosion rates to inform restoration prioritisation, and to monitor effectiveness of gully restoration, has employed the use of remotely sensed spatial data. This includes LiDAR from terrestrial lidar scanners (TLS), airborne and unmanned aerial vehicle (UAV)-based lidar surveys, and more recently handheld laser scanners (HLSs) (Kinsey-Henderson et al. 2021). LiDAR sensors capture data in the form of a point cloud, where each point has X, Y, and Z coordinates. Together, these points create a three-dimensional representation of the scanned environment or features. Advances in HLS technology have resulted in devices that boast near-TLS accuracy while being highly portable, provide a more even point density distribution, and are a quicker and easier data acquisition method for capturing environments with high surface complexity (Frangez et al. 2018; Kinsey-Henderson et al. 2021; Stroner et al. 2025).

As with any sensor, HLS are subject to error. The compounding positional error in an HLS is referred to as “drift”. Drift is both sensor and environment-dependent (Kinsey-Henderson et al. 2021), with detections of drift ranging from 0.1 m to above 1 m being documented in point clouds captured with commercial HLS in underground mines (e.g. Frangez et al. 2018; Raval et al. 2019; Stroner et al. 2025), urban environments and civil infrastructure (e.g. Keitaanniemi et al. 2020; Keitaanniemi et al. 2023) and outdoor cultural heritage sites (Zlot et al. 2014). There are limited papers documenting drift in HLS in geomorphic environments, specifically in gullies. Kinsey-Henderson et al. (2021) assessed the accuracy of HLS relative to TLS and Real-Time Kinematic (RTK) GPS surveys for measuring gully attributes (gully volume, area and maximum depth), however the study did not assess the HLS sensor drift as a function of time. Understanding the expected margin of error helps determine the maximum duration for gully monitoring scans and establishes the threshold at which recorded geomorphic changes can be attributed to sediment loss with confidence, rather than to measurement uncertainty

Measuring drift in the point cloud can prove challenging where noise around a refence object, such as a sphere, inhibits the ability to accurately select and measure distances between individual points in the point cloud. Rather than attempting this, drift in this study was measured in the trajectory of the sensor, as this is ultimately where drift error arises. It is anticipated that the ability of the sensor to accurately measure the distance between itself and an object does not change notably overtime, but the ability of the sensor to keep track of its position is subject to compounding error. Upon processing, the HLS data produces a separate trajectory file with timestamped local coordinates of the sensor’s heading relative to the start location. The difference between the sensor’s recorded position in the trajectory file at a single control point at two periods during each data acquisition scan was used to quantify drift.

The HLS used in this study was a SLAM (Simultaneous Localization and Mapping) device. The SLAM algorithm uses input from the measurement sensor (in this case a LiDAR sensor) and from the motion sensor (the inertial measurement unit) to build a three-dimensional map of an environment whilst computing the position of the sensor within the constructed map. These steps are interdependent: the motion model predicts the sensor’s position using motion sensor inputs, while the observation model refines this estimate based on detected features (Abdulmajeed and Mansoor, 2024).

This study assessed drift in a commercially available SLAM scanner in a channel gully during non-georeferenced closed loop scans, where “closed loop” refers to starting and finishing the scan at the same position. An optimal gully to capture with a SLAM-based HLS is a multilobed gully, where the scanned path, due to the shape of the gully, includes closed loops, which allow the SLAM algorithm to reduce the drift accumulated (Geoslam ZEB Horizon User Guide, 2022). A channel-type gully was intentionally selected for the study as it allowed for testing the HLS under suboptimal conditions; where the survey path was a “there and back” loop that by default does not include closed loops during data collection.

The aims of this study were to:

1) determine the relationship between data acquisition/scan time and drift; and
2) determine the efficacy of incorporating closed loops into a survey for reducing drift.

2. METHODS

2.1. Device used

The SLAM HLS sensor used was the GeoSLAM ZEB Horizon, which incorporates a Velodyne puck (VLP-16 Lite) LiDAR sensor (

Figure 1 GeoSLAM ZEB Horizon on a control point

Figure 2 The study site

. The sensor features 16 channels, a 100 m range, a 360º x 270º field of view, a scan noise range of ± 30 mm and is capable of registering 300 000 points per second. The scanner was used with the reference base fitted to allow placing the sensor on control points.

Figure 1 GeoSLAM ZEB Horizon on a control point

Figure 2 The study site

2.2. Study site and data acquisition method

The study site was a channel-like gully (**Error! Reference source not found.**) located near Duaringa, Queensland, Australia. In July 2025, 48 individual scans of the gully were undertaken. Scans were conducted in sets of eight scans of durations from 5 to 40 minutes (Table 1). The procedure was repeated three times under each treatment: resulting in three sets of scans each with and without mid-loop scans. Scans were conducted at walking pace, which was kept as consistent as possible (between 12-16 minutes per km; measured using a Garmin Instinct GPS watch). Scans were undertaken by walking from the start/stop control point for half of the scan duration, then turning 180 degrees and returning along the same route in reverse, to the start/stop control point.

2.3. Trajectory control points

Concrete pavers were used as trajectory control points for each scan, which the reference base of the ZEB Horizon was placed onto. Scans were started and stopped at the start/stop control point. Preliminary testing suggested the greatest drift would occur where the outbound and inbound midpoints intersect. As such, a mid-scan control point was established halfway along the length of the outbound leg of the scan; the sensor was placed on the control point for approximately 20 seconds at both a quarter and three quarters into the scan duration (prompting the sensor to record these as “stop and go georeference points”).

2.4. Closed loops

Scans with mid-scan loops were performed by walking a loop of approximately four metres in diameter, at five-minute intervals and a double loop halfway through the scan duration (at the turn around point). The five- and ten-minute scans in these sets had double loops at the turn around point only. Closed loops were not performed for scans with mid-scan loops.

Table 1 Scan durations comprising one set

Scan	Approximate duration (min)	Scan	Approximate duration (min)
Scan 1	5	Scan 5	25
Scan 2	10	Scan 6	30
Scan 3	15	Scan 7	35
Scan 4	20	Scan 8	40

2.5. Data processing and analysis

Point clouds and trajectory files were retrieved from the sensor and processed using the “Process SLAM” workflow with “standard” i.e. closed loop capture environment workflow in Faro Connect v2024.3.5. Default settings were adopted for all other inputs. The “Registration” function in Faro Connect was used to identify the timestamps associated with the sensor being placed on the mid-scan control points, noting point clouds were not georeferenced for this study. Lateral (x), longitudinal (y) and height (z) were extracted from the trajectory text (.txt) file for each scan. These vectors were used to calculate a Euclidean distance[1]. The difference between Euclidean distances was used to determine start/end trajectory drift (the displacement between the sensor’s recorded location at the start and the end of the scan at the start/end control point), and the mid-scan trajectory drift (the displacement between the sensor’s recorded location a quarter of the way and three quarters of the way through the scan duration at the mid-scan control point). Scatter plots were generated, and Spearman’s correlation analysis (rho) was run using R (v4.3.2). Drift severity was classified as per **Error! Reference source not found.**, noting that this is subjective to the user and intended data use. For this study, a 0.1 m resolution is adopted when exporting .las files, and the data at this resolution is used to detect change in gullies and streambanks in the Fitzroy catchment over several years where change in the order of tens of centimetres to a few metres is typical (e.g. headcut migration). The Geoslam ZEB Horizon User Guide (2022) recommends scan duration is limited to 30 minutes to reduce drift. For this reason, the drift severity for scans below and above 25 minutes was assessed.

Table 2 Drift severity classification

Trajectory drift	Classification of drift severity[2]
<0.1 m	Negligible
0.1 – 0.15 m	Acceptable
0.15 – 0.5 m	Moderate
>0.5 m	Excessive

[1] Using the formula $d = \sqrt{[(x2 - x1)^2 + (y2 - y1)^2 + (z2 - z1)^2]}$, where (x1, y1, z1) are the coordinates of the first point and (x2, y2, z2) are the coordinates of the second point

[2] Scans could only meet one scan severity class; the more severe class being adopted in instances where two applied.

2.6. Assumptions/limitations

The study did not involve a comparison against independent reference measurements, and did not seek to quantify drift in georeferenced scans.

The methodology for data acquisition did not adhere to best use guidelines per the manufacturer's recommendations to allow for the SLAM algorithm to keep track of the sensor position (Geoslam ZEB Horizon User Guide, 2022). That is, certain scans deliberately exceeded the maximum recommended duration of 25 minutes and "there and back" scans without the mid-scan loops were conducted, which is not recommended by the manufacturer. This was done to develop an understanding of likely scan degradation in the real world if duration and scan path varied from these recommendations.

3. RESULTS

The data from the study (Figure 3) showed non-significant relationships between scan duration and drift in scans without mid-scan loops at the start/stop control point (rho = 0.19, n= 24, P = 0.38), the mid-scan control point (rho = -0.11, n = 24, P = 0.61), and in scans with mid-scan loops at the start/stop control point (rho = 0.16, n = 24, P = 0.45) and the mid-scan control point (rho= 0.19, n = 24, P= 0.38).

Excessive drift (> 0.5 m) was only recorded at the mid-scan control points, the largest drift was 2.57 m during a 24 min scan; the maximum drift at the start/stop control points was deemed acceptable (0.13 m during a 31 min scan). Across all scans 76% had negligible drift, 8% had acceptable drift and 15% had excessive drift. No scans recorded drift in the moderate range.

When scan duration was below 25 minutes, 92% of scans had negligible drift, 4% had acceptable drift and 4% of scans had excessive drift (Figure). When scan duration exceeded 25 minutes, 57% of scan had negligible drift, 14% had acceptable drift and 29% of scans had excessive drift (Figure).

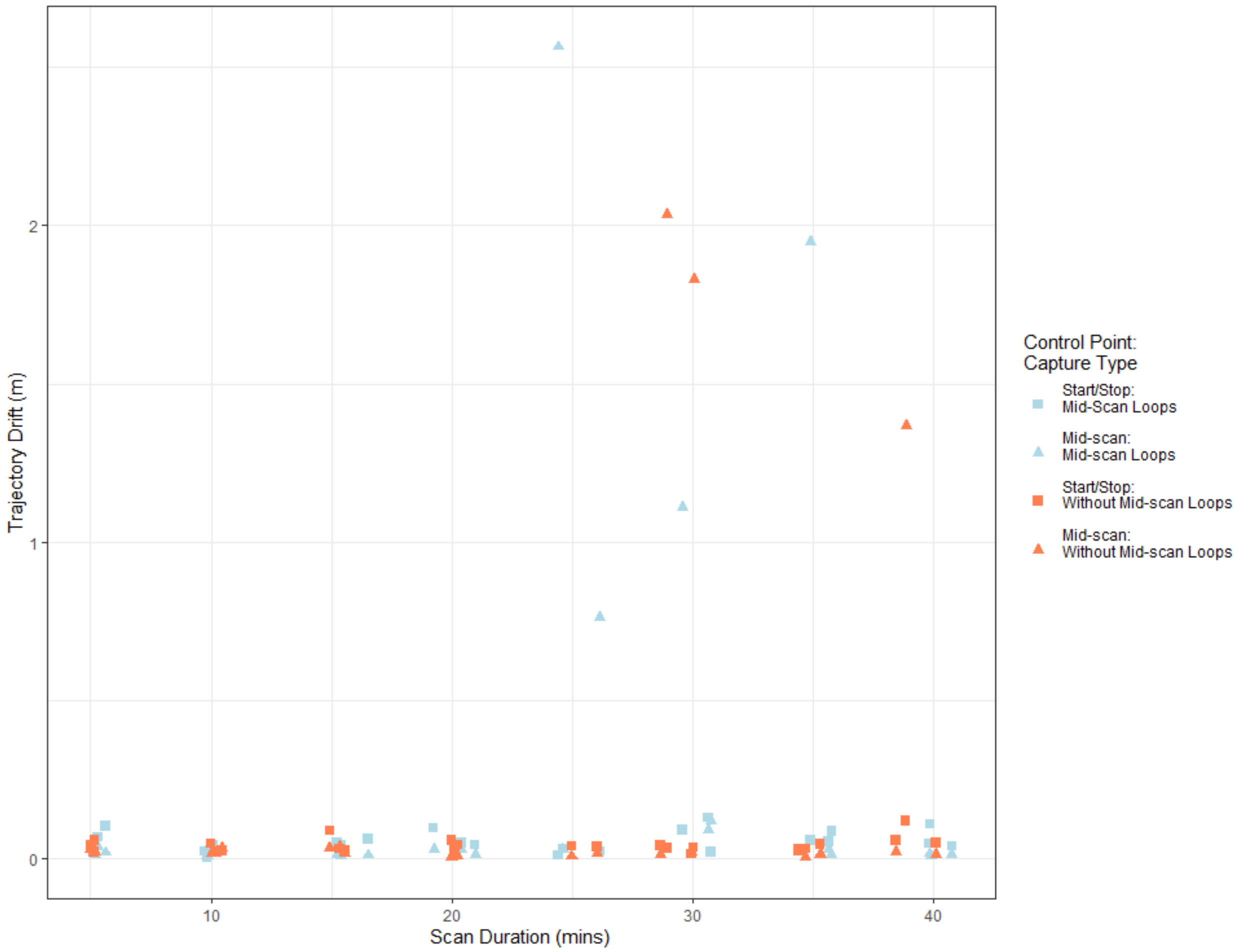

Figure 3. Trajectory drift across all scans

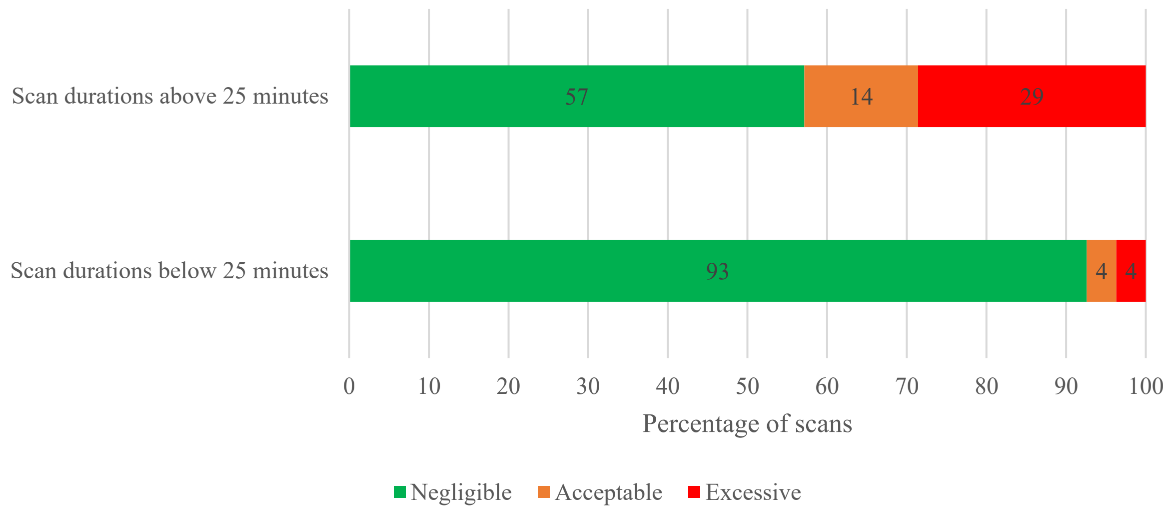

Figure 4. Drift severity in scans with durations below and above 25 minutes

4. DISCUSSION AND CONCLUSION

The results of the study indicate no statistically significant correlation between scan duration and trajectory drift at the control points in scans both with and without mid-scan loops. However, when scans exceeded 25 minutes in duration, the probability of introducing excessive drift increased. Despite this, 71% of the scans exceeding 25 minutes still had negligible or acceptable levels of drift, and no scans were deemed to have moderate drift. Of the longest duration scans (~ 40 minutes), 83% had drift within negligible or acceptable levels. The SLAM algorithm, when running the closed loop workflow in Faro Connect, largely corrected for the drift at the start/end of the scans and no excessive drift was recorded at the start/end control point. A user can override some of this drift correction by processing a closed loop scan with the open loop workflow; this results in displacement of the trajectory at the end relative to the start position and the "mirroring" of features near the end of the scan because of the trajectory drift. One would therefore anticipate minimal drift at the start/end of the scans in this study. However, the lack of consistent excessive drift in longer scans at the mid-scan control points was surprising and not consistent with preliminary testing. During preliminary unreported testing, drift in the order of 1.5 m was consistently observed in the trajectory and point cloud for "there and back" scans without mid-scan control points with durations longer than 35 minutes at approximately the one quarter/three quarter duration location.

A variable other than scan duration was responsible for introducing excessive drift at the mid-scan control points in certain scans beyond 25 minutes. This could potentially be a lack of appropriate features within range of the mid-scan control points for these particular scans. The results cannot be used to adequately determine the relationship between duration and drift nor the efficacy of closed loops at reducing drift and an alternative design is required to test both aims of this study.

It is hypothesised that mid-scan control points give the sensor two opportunities per scan to capture a high point cloud density of common features. This, in turn, enables the SLAM algorithm to correct trajectory drift that would otherwise occur at those locations. Evaluating the effectiveness of mid-scan control points in reducing drift, compared to traditional closed loops, is worthwhile, as this may offer an alternative drift-reduction method in environments where closed loops are impractical, such as confined gullies with only a narrow walkable floor.

ACKNOWLEDGMENTS

We acknowledge our colleagues in the Rockhampton DETSI Paddock to Reef team for their advice and input.

REFERENCES

Abdulmajeed W and Mansoor R. (2014). Visual Robot SLAM of 2D & 3D Indoor Environment. LAP LAMBERT Academic Publishing, London.

Bartley R, Bainbridge Z T, Lewis S E, Kroon F J, Wilkinson S N, Brodie J E and Silburn D M (2014). Relating sediment impacts on coral reefs to watershed sources, processes and management: A review. Science of the Total Environment, 468–469, 1138–1153.

Frangez V, Kramis B, Hübscher F and Baumann A (2018) Comparison of three innovative technologies for 3D-acquisition, modelling, and visualization of an underground mine, in: Online Proceedings, International Federation of Surveyors (FIG), 2018, p. 9502.

Geoslam ZEB Horizon User Guide V4.0, 2022, https://tinyurl.com/m5yvfmn6. Accessed on 19 August 2024.

Keitaanniemi A, Rönnholm P, Kukko A and Vaaja M T (2023) Drift analysis and sectional post-processing of indoor simultaneous localization and mapping (SLAM)-based laser scanning data. Automation in Construction 147, 104700.

Keitaanniemi A, Kukko A, Virtanen J P and Vaaja M T (2020) Measurement strategies for street-level SLAM laser scanning of Urban environments, The Photogrammetric Journal of Finland 27, 1-19.

Koci J, Sidle RC, Jarihani B, Cashman MJ (2020) Linking hydrological connectivity to gully erosion in savanna rangelands tributary to the Great Barrier Reef using structure-from-motion photogrammetry. Land Degradation and Development 31, 20–36.

Lamane H, Mouhir L, Zouahri A, Baghdad B, El Bilali A, Moussadek R (2025) Modeling soil erosion and sediment yield under climate change: a comparison of RUSLE and MUSLE integrated with SDR using variable soil data resolutions. Modeling Earth Systems and Environment 11(5):343.

Raval S, Banerjee B P, Kumar Singh S, Canbulat I (2019) A preliminary investigation of mobile mapping technology for underground mining. IGARSS 2019 - 2019 IEEE International Geoscience and Remote Sensing Symposium, 6071–6074

Štroner M, Urban R, Křemen T et al (2025) Scanning the underground: comparison of the accuracies of SLAM and static laser scanners in a mine tunnel. Journal of the International Measurement Confederation 242:115875

Waterhouse J, Pineda M-C, Sambrook K, Newlands M, McKenzie L, Davis A, Pearson R, Fabricius K, Lewis S, Uthicke S, Bainbridge Z, Collier C, Adame F, Prosser I, Wilkinson S, Bartley R, Brooks A, Robson B, Diaz-Pulido G, Reyes C, Caballes C, Burford M, Thorburn P, Weber T, Waltham N, Star M, Negri A, Warne M, S,J., Templeman S, Silburn M, Chariton A, Coggan A, Murray-Prior R, Schultz T, Espinoza T, Burns C, Gordon I, Devlin M (2024) 2022 Scientific Consensus Statement: Conclusions.

Zlot R, Bosse M, Greenop K, Jarzab Z, Juckes E, Roberts J (2014) Efficiently capturing large, complex cultural heritage sites with a handheld mobile 3D laser mapping system. Journal of Cult Heritage 15(6):670–678.